AFRL-AFOSR-VA-TR-2015-0242

ULTRACOLD FERMIONS IN THE P-ORBITAL BAND OF AN OPTICAL LATTICE

Kenneth O'Hara
PENNSYLVANIA STATE UNIVERSITY

07/29/2015
Final Report

Air Force Research Laboratory
AF Office Of Scientific Research (AFOSR)/ RTB
Arlington, Virginia 22203
Air Force Materiel Command

REPORT DOCUMENTATION PAGE

Form Approved
OMB No. 0704-0188

PLEASE DO NOT RETURN YOUR FORM TO THE ABOVE ORGANIZATION.

1. REPORT DATE *(DD-MM-YYYY)*	2. REPORT TYPE	3. DATES COVERED *(From - To)*
27-07-2015	Final	15 July 2011 - 31 March 2015

4. TITLE AND SUBTITLE
Ultracold Fermions in the P-Orbital Band of an Optical Lattice

5a. CONTRACT NUMBER

5b. GRANT NUMBER
FA9550-11-1-0161

5c. PROGRAM ELEMENT NUMBER

6. AUTHOR(S)
Kenneth M. O'Hara

5d. PROJECT NUMBER

5e. TASK NUMBER

5f. WORK UNIT NUMBER

7. PERFORMING ORGANIZATION NAME(S) AND ADDRESS(ES)
PENNSYLVANIA STATE UNIVERSITY, THE
PENN STATE
408 OLD MAIN
UNIVERSITY PARK PA 16802-1505

8. PERFORMING ORGANIZATION REPORT NUMBER

9. SPONSORING/MONITORING AGENCY NAME(S) AND ADDRESS(ES)
USAF, AFRL DUNS 143574726
AF OFFICE OF SCIENTIFIC RESEARCH
875 N. RANDOLPH ST. ROOM 3112
ARLINGTON VA 22203

10. SPONSOR/MONITOR'S ACRONYM(S)

11. SPONSOR/MONITOR'S REPORT NUMBER(S)

12. DISTRIBUTION/AVAILABILITY STATEMENT
Approved for public release; Distribution is unlimited

13. SUPPLEMENTARY NOTES

14. ABSTRACT

The goal of this research program is to investigate strongly-correlated many-body phases that emerge when interacting fermions occupy the p-orbital band of an optical lattice. Progress made toward this objective included demonstration of a site-resolved, continuously deformable two-dimensional honeycomb/triangular lattice and loading of Li-6 atoms into a triangular configuration of lattice beams. Further, a novel solid state laser source for 671 nm light was developed and new methods for rapidly controlling interactions between fermionic Li-6 atoms were demonstrated. While making this progress, scientific opportunities arose to make discoveries in other research areas of interest to the AFOSR. Specifically, the scope of the project was broadened to include studies of s-wave collisional frequency shifts in an ultracold Fermi gas (relevant for improving/characterizing the accuracy of next generation atomic clocks), the realization of momentum dependent s-wave interactions in a Fermi gas (relevant for quantum simulation), and the realization of multi-partite entangled states by dissipative exothermic collisions in a one-dimensional Fermi gas (relevant for quantum metrology).

15. SUBJECT TERMS
Fermi Gas; Optical Lattice; Ultracold Collisions; Atomic Clock; Fano-Feshbach Resonance; Strongly-Correlated Systems

16. SECURITY CLASSIFICATION OF:			17. LIMITATION OF ABSTRACT	18. NUMBER OF PAGES	19a. NAME OF RESPONSIBLE PERSON
a. REPORT	b. ABSTRACT	c. THIS PAGE			19b. TELEPHONE NUMBER *(Include area code)*
U	U	U	UU		

INSTRUCTIONS FOR COMPLETING SF 298

1. REPORT DATE. Full publication date, including day, month, if available. Must cite at least the year and be Year 2000 compliant, e.g. 30-06-1998; xx-06-1998; xx-xx-1998.

2. REPORT TYPE. State the type of report, such as final, technical, interim, memorandum, master's thesis, progress, quarterly, research, special, group study, etc.

3. DATES COVERED. Indicate the time during which the work was performed and the report was written, e.g., Jun 1997 - Jun 1998; 1-10 Jun 1996; May - Nov 1998; Nov 1998.

4. TITLE. Enter title and subtitle with volume number and part number, if applicable. On classified documents, enter the title classification in parentheses.

5a. CONTRACT NUMBER. Enter all contract numbers as they appear in the report, e.g. F33615-86-C-5169.

5b. GRANT NUMBER. Enter all grant numbers as they appear in the report, e.g. AFOSR-82-1234.

5c. PROGRAM ELEMENT NUMBER. Enter all program element numbers as they appear in the report, e.g. 61101A.

5d. PROJECT NUMBER. Enter all project numbers as they appear in the report, e.g. 1F665702D1257; ILIR.

5e. TASK NUMBER. Enter all task numbers as they appear in the report, e.g. 05; RF0330201; T4112.

5f. WORK UNIT NUMBER. Enter all work unit numbers as they appear in the report, e.g. 001; AFAPL30480105.

6. AUTHOR(S). Enter name(s) of person(s) responsible for writing the report, performing the research, or credited with the content of the report. The form of entry is the last name, first name, middle initial, and additional qualifiers separated by commas, e.g. Smith, Richard, J, Jr.

7. PERFORMING ORGANIZATION NAME(S) AND ADDRESS(ES). Self-explanatory.

8. PERFORMING ORGANIZATION REPORT NUMBER. Enter all unique alphanumeric report numbers assigned by the performing organization, e.g. BRL-1234; AFWL-TR-85-4017-Vol-21-PT-2.

9. SPONSORING/MONITORING AGENCY NAME(S) AND ADDRESS(ES). Enter the name and address of the organization(s) financially responsible for and monitoring the work.

10. SPONSOR/MONITOR'S ACRONYM(S). Enter, if available, e.g. BRL, ARDEC, NADC.

11. SPONSOR/MONITOR'S REPORT NUMBER(S). Enter report number as assigned by the sponsoring/ monitoring agency, if available, e.g. BRL-TR-829; -215.

12. DISTRIBUTION/AVAILABILITY STATEMENT. Use agency-mandated availability statements to indicate the public availability or distribution limitations of the report. If additional limitations/ restrictions or special markings are indicated, follow agency authorization procedures, e.g. RD/FRD, PROPIN, ITAR, etc. Include copyright information.

13. SUPPLEMENTARY NOTES. Enter information not included elsewhere such as: prepared in cooperation with; translation of; report supersedes; old edition number, etc.

14. ABSTRACT. A brief (approximately 200 words) factual summary of the most significant information.

15. SUBJECT TERMS. Key words or phrases identifying major concepts in the report.

16. SECURITY CLASSIFICATION. Enter security classification in accordance with security classification regulations, e.g. U, C, S, etc. If this form contains classified information, stamp classification level on the top and bottom of this page.

17. LIMITATION OF ABSTRACT. This block must be completed to assign a distribution limitation to the abstract. Enter UU (Unclassified Unlimited) or SAR (Same as Report). An entry in this block is necessary if the abstract is to be limited.

A Objectives

The original goal of this research program was to investigate strongly-correlated many-body phases that emerge when interacting fermions occupy the p-orbital band of an optical lattice. The behavior of atoms in the p-band of an optical lattice is markedly different from that observed for atoms in the s-band. Most notably, population of the p-orbital band introduces (1) a new degree of freedom due to orbital degeneracy and (2) a tunneling anisotropy which depends on the orientation of the orbital wavefunction. By investigating orbital physics in the well-controlled environment provided by fermionic atoms in an optical lattice, we hope to better understand orbital physics at play in condensed matter systems such as the transition metal oxides and the recently discovered superconducting iron-pnictides. The physical properties of strongly correlated phases in the transition metal oxides and iron pnictides are determined by the complicated interplay of charge, spin and orbital degrees of freedom. The system we study allows for each of these degrees of freedom to be added individually, in pairs, or all at once, permitting a much more systematic investigation of the role that orbital physics plays in determining the properties of strongly-correlated Fermi systems. Progress toward these goals was made during this grant period though not all of the original objectives were achieved. The study of p-orbital band physics in a lattice gas remains an enduring goal of this ongoing research program.

While making progress toward the objectives described above, scientific opportunities arose to make discoveries using the same experimental apparatus in other research areas that are of interest to the AFOSR. Specifically, the scope of the project was broadened to include studies of s-wave collisional frequency shifts in an ultracold Fermi gas (relevant for improving/characterizing the accuracy of next generation atomic clocks), the realization of momentum dependent s-wave interactions in a Fermi gas (relevant for quantum simulation), the rapid control of interactions in a ^{6}Li Fermi gas (relevant for characterizing strongly correlated phases of ultracold matter), the realization of multi-partite entangled states by dissipative exothermic collisions in a one-dimensional Fermi gas (relevant for quantum metrology), and the observation of the Fulde-Ferrell-Larkin-Ovchinikov phase in a 1D Fermi gas (relevant for understanding exotic paired superconducting phases).

B Accomplishments/New Findings

B.1 Observation of s-Wave Collisional Frequency Shift in a Fermi Gas

An original objective of our research program was to use a narrow p-wave Feshbach resonance in ^{6}Li to induce repulsive interactions in a spin polarized Fermi gas and observe Wigner crystallization of atoms in the lowest p-orbital band of a honeycomb lattice. Using the narrow p-wave Feshbach resonance in ^{6}Li [1] to control interactions, however, requires exceptional magnetic field stability. We improved the field stability of our system such that the measured root-mean-square fluctuations of our field is now less than $250\,\mu$G at a bias field of $528\,$G. Having attained such a stringent control over our magnetic field, we realized that we were uniquely positioned to make the first definitive observation and characterization of an s-wave collisional frequency shift of a clock transition in an ultracold Fermi gas. Such a shift is of direct relevance for next generation atomic clocks which make use of fermionic isotopes of alkaline earth atoms in an attempt to minimize such shifts. However, an s-wave collisional frequency shift (sCFS) in a Fermi gas had not been definitively observed or characterized prior to our work; what had been thought to be an sCFS in a Sr optical lattice clock [2] could in fact be explained by p-wave collisional frequency shifts [3].

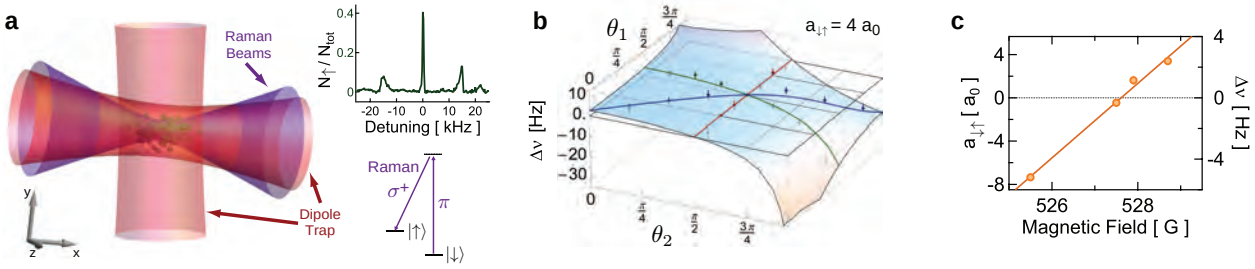

Figure 1: Observation of the s-wave collisional frequency shift (sCFS) of a spin-1/2 Fermi gas. (a) To measure the collisional frequency shift in a ^{6}Li gas, we begin with a spin-polarized Fermi gas and drive a spatially inhomogeneous two-photon Raman transition using focused co-propagating beams. (Inset: The clock transition is operated in the resolved sideband limit.)
(b) The sCFS as a function of first (θ_1) and second (θ_2) pulse area in Ramsey interferometry. Comparison between the measured sCFS and that predicted by Gibble [4]. The agreement is excellent with only a single free parameter to account for our uncertainty in absolute atom number.
(c) The sCFS tunes and changes sign with the s-wave scattering length a.

At low enough temperatures that p-wave collisions are frozen out, a spin-polarized Fermi gas is not interacting as the exclusion principle forbids s-wave collisions between identical fermions. Even if all the atoms are in superposition states, the fermions still do not collide provided that all of the atoms are in precisely the same superposition state. For this reason, it had been believed that collisional frequency shifts, which are a primary limitation to the accuracy of our current primary frequency standards, could be eliminated in atomic clocks if ultracold fermionic atoms were used [5, 6]. Indeed, an MIT experiment suggested that two component Fermi gases were universally immune to such shifts given that no shift was observed for an incoherent two-component imbalanced spin mixture [7]. In 2009 it was suggested, however, that cold collisional shifts could

occur for a Fermi-based atomic clock if the electromagnetic field used to probe the atoms was spatially inhomogeneous [2,4,8,9]. In this case, due to the spatial inhomogeneity of the field, atoms in different quantum states of the trap would experience different Rabi frequencies and even a gas of initially spin-polarized fermions would be made distinguishable by the probe field. Inhomogeneity of the probe field is particularly relevant for next generation optical lattice clocks which make use of optical transitions because the field varies on the scale of an optical wavelength. Thus, observing and characterizing such shifts is important for the development of optical lattice clocks so that the shifts can be minimized to the extent possible and properly included in an error budget. However, analytical expressions that purported to predict the behavior of the sCFS in an ultracold fermionic gas were mutually incompatible [2,4]. By driving a clock transition in a gas of fermionic ^{6}Li atoms with a spatially inhomogeneous pair of Raman beams, we were able to definitively observe and characterize an sCFS in an ultracold Fermi gas for the first time.

We used the two lowest hyperfine states in ^{6}Li (states $|\downarrow\rangle$ and $|\uparrow\rangle$) as our clock states which, at a bias magnetic field of $528\,\mathrm{G}$, have a transition frequency of $76\,\mathrm{MHz}$. If a spatially homogeneous radio-frequency field was used to excite the transition as in the MIT experiments [6, 7], no collisional frequency shift was observable. However, we introduced a spatially inhomogeneous excitation by driving the $|\downarrow\rangle - |\uparrow\rangle$ transition with a pair of co-propagating Raman fields that were focussed to a waist that was comparable to the size of the atomic cloud (see Fig. 1(a)). The inhomogeneity of the field, calibrated by the dephasing rate of Rabi oscillations, was controllable and could be made comparable to the inhomogeneity existing in state-of-the-art optical lattice clocks [2]. To accurately mimic optical lattice clock experiments and have a system modeled by the theory that describes them [2, 4, 8, 9], we worked in the resolved sideband regime for our clock transition and we studied a weakly interacting gas so that trap state changing collisions could be ignored over the time scale of the experiment. We used Ramsey interferometry to characterize the sCFS as this could most directly distinguishes between the competing analytic predictions for the shift [2, 4].

The sCFS for fermions behaves dramatically different from that observed for bosons. The sCFS for bosons arises from the difference in mean field interaction shifts for populations in the two clock states and thus the shift is proportional to the difference in partial densities ($\rho_\uparrow - \rho_\downarrow$) during the free evolution time in a Ramsey interferometer. For bosons, the sCFS would be observed to go to zero for a first pulse area $\theta_1 = \pi/2$ since this would make $\rho_\uparrow - \rho_\downarrow = 0$ during the free evolution time. In Ref. [2] it was assumed that the sCFS for fermions would also be proportional to the difference in partial densities. We have shown experimentally that this is not the case. Strikingly, the sCFS for fermions is relatively insensitive to θ_1 (see Fig. 1(b)) and specifically does not go through zero for $\theta_1 \approx \pi/2$. Instead the sCFS for fermions is sensitive to the second pulse area θ_2 and goes through zero for $\theta_2 \approx \pi/2$ (see Fig. 1(b)).

The qualitative behavior of the sCFS for fermions can be understood already in a two atom model [4]. A good set of basis states for the two atom model are the spin triplet and singlet states. The singlet state has a symmetric two-body spatial wavefunction and experiences an interaction shift whereas the triplet states do not. For initially spin polarized atoms, an inhomogeneous field is necessary in order to couple the initial spin polarized triplet state $|\downarrow\downarrow\rangle$ to the singlet state if a shift is to be observed. Also, if a shift is to be observed, the second pulse of the Ramsey

interferometer needs to be inhomogeneous in order to again couple singlet and triplet states so that the phase acquired by the singlet state during the free evolution time can interfere with the phase of the unshifted triplet states. An explicit expression for the shifts can be derived by solving the Schrödinger equation assuming the pulses of the interferometer are short [4]. This yields:

$$\Delta\nu = \frac{g}{\pi\mathcal{A}} \sin(2\Delta\theta_1) \sin(\Delta\theta_2) \cos(\bar{\theta}_2).$$

Here, $2g$ is the interaction shift of the singlet state which is proportional to the s-wave scattering length, $\mathcal{A}$ is the amplitude of the Ramsey fringe, $\Delta\theta_i$ is the difference in pulse areas for the two atoms due to the inhomogeneity and $\bar{\theta}_i$ is the average pulse area for the two atoms. Note that the shift is predicted to go through zero for $\bar{\theta}_2 = \pi/2$. Physically the sCFS goes through zero for $\theta_2 = \pi/2$ because the two atoms experience frequency shifts that are equal in magnitude but opposite in sign and, if their phases are read out with equal sensitivity which occurs when $\bar{\theta}_2 = \pi/2$, the frequency shifts cancel. For many atoms, the collisional frequency shift becomes:

$$\Delta\nu = \frac{\sum_{\text{pairs}} g_{\alpha\beta} \sin(2\Delta\theta_{1,\alpha\beta}) \sin(\Delta\theta_{2,\alpha\beta}) \cos(\bar{\theta}_{2,\alpha\beta})}{\pi\mathcal{A}}$$

For comparison, this expression is plotted as the 3D surface in Fig. 1(b) with only a single free overall scaling factor adjusted to account for our uncertainty in the absolute number calibration. The sCFS is relatively insensitive to θ_1 and does go through zero near $\theta_2 = \pi/2$. Notably, however, correlations in the gas, between the interaction shift $2g_{\alpha,\beta}$ and the average Rabi frequencies $\bar{\Omega}_{\alpha\beta}$ for example, can shift the location of the zero crossing of the sCFS slightly away from $\theta_2 = \pi/2$. It is interesting to note that current state-of-the-art optical lattice clocks using fermionic atoms can have collisional frequency shifts due to both s-wave and p-wave collisions [3, 10]. Ref. [3] experimentally showed that p-wave collisional frequency shifts for fermions behave like s-wave collisional frequency shifts for bosons and can typically be eliminated by adjusting the first pulse area around $\theta_1 = \pi/2$. Our work shows that the s-wave collisional frequency shift can be eliminated by adjusting the second pulse area around $\theta_2 = \pi/2$. Thus, it should be possible to operate optical lattice clocks at a point where both s-wave and p-wave collisional shifts are simultaneously eliminated. Our work was described in an article appearing in *Physical Review Letters* [11].

B.2 Realization of a Resonant Fermi Gas with a Large Effective Range

The superb field stability of our system also allowed for a precision study of the narrow s-wave Feshbach resonance in ^{6}Li which occurs for the two lowest energy hyperfine states at a field of $543.3\,\mathrm{G}$. In contrast to a broad resonance, such as the extensively studied resonance occurring in ^{6}Li for this mixture at $832\,\mathrm{G}$, the molecular state associated with a narrow resonance is only weakly coupled to free particles in the continuum. The energy scale associated with this coupling is much smaller than van der Waals energy scale and can be smaller or comparable to the Fermi energy at densities typical found in ultracold gas experiments. The existence of this new energy scale which can be comparable to the Fermi energy means that effective interaction potential for the atoms has an energy dependence on the scale of the Fermi energy. Thus, this interaction potential cannot be described simply by a zero-range or contact potential parameterized by a single parameter – the s-wave scattering length a. Instead, the effective interaction potential behaves as though

it has a finite range and at least two parameters are required to describe the s-wave scattering phase shift at low energy – within the resonance these are the the s-wave scattering length a *and* the effective range $r_{\rm eff}$. We showed experimentally that near the narrow resonance in ^{6}Li, the interactions in the gas cannot be described simply by a contact potential. Rather the interactions had an energy dependence for relative collision energies much less than the van der Waals energy. We found that at resonance, the effective range for this resonance $r_{\rm eff} = -7 \times 10^4\, a_0$ which can be comparable to or larger than $1/k_F$ where k_F is the Fermi wavenumber in typical dilute gas systems.

Well within the narrow Feshbach resonance, the low energy expansion of the s-wave scattering phase shift δ is given by

$$k \cot(\delta) = -\frac{1}{a} + \frac{1}{2} r_{\rm eff} k^2 + ...$$

where the scattering length a is given by

$$a = a_{\rm bg} \frac{\Delta}{B_\infty - B}$$

and the effective range $r_{\rm eff}$ is given by

$$r_{\rm eff} = -\frac{2\hbar^2}{m} \frac{1}{a_{\rm bg} \gamma \Delta}$$

where $a_{\rm bg}$ is the background scattering length, Δ is the width of the resonance in Gauss, B_∞ is the resonance location in Gauss, and γ is the difference between the magnetic dipole moments of the bound molecular state and the two free atoms in the continuum. Note that the effective range $r_{\rm eff} \propto 1/\Delta$.

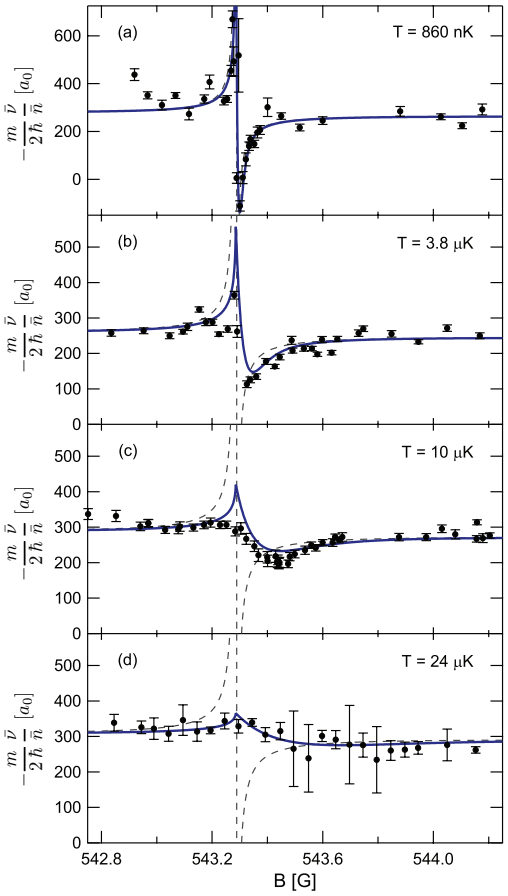

Figure 2: Observation of interaction shifts by radio-frequency spectroscopy near the narrow Feshbach resonance in ^{6}Li. The interaction shift of the $|\uparrow\rangle - |3\rangle$ transition is plotted as a function of field in the vicinity of the narrow resonance at $543.3\,\mathrm{G}$ for gasses at different temperatures ($860\,\mathrm{nK}$ (a), $3.8\,\mu\mathrm{K}$ (b), $10\,\mu\mathrm{K}$ (c), $24\,\mu\mathrm{K}$ (d)) which show a dramatic dependence on temperature even though all temperatures are well below the van der Waals energy scale $E_{\rm vdW}/k_B = 29.5\,\mathrm{mK}$. The prediction for a contact potential is shown as a dashed line and a mean field prediction including the expected energy dependence for a narrow resonance is shown as the solid curves.

An important motivation for this work is to expand upon the types of interactions that can be considered in the quantum simulation of strongly correlated matter. For example, an accurate quantum simulation of the equation of state of neutron matter requires

a system in which the s-wave scattering length is much larger than the average interparticle spacing but also the effective range is at least comparable to the average interparticle spacing [12]. The equation of state of a unitary Fermi gas that has been recently measured to high accuracy [13] would only be relevant for neutron densities where $k_F\, r_{\rm eff} \ll 1$ for neutron matter so that the effective range can be safely ignored. However, this requires that the neutron matter density is less than the neutron drip density below which neutrons become unbound. A more accurate equation of state requires that $k_F\, r_{\rm eff} \gtrsim 1$ [12].

To show that a Fermi gas near a narrow Feshbach resonance cannot be simply described by a contact interaction parameterized by only the s-wave scattering length, we measured the interaction energy in the gas via radio-frequency spectroscopy with an auxiliary hyperfine state (state $|3\rangle$) at different temperatures (see Fig. 2). The interaction shift data show a striking temperature dependence even though all of the temperatures are well below the van der Waals energy scale $E_{\rm vdW}/k_B = 29.5\,{\rm mK}$. At the lowest temperature, the data can be fit by the prediction for a contact potential parameterized by a field dependent scattering length (dashed line in Fig. 2) or a mean-field description that includes the energy dependence of the scattering phase shift expected for a narrow resonance (solid line in Fig. 2). If the same parameters determined from the low temperature fit are used to predict the behavior at higher temperatures, however, the contact potential model is a poor description of the data whereas the model which includes the energy dependence of a narrow resonance provides a good description. The fact that the mean-field model which accounts for the expected energy dependence can deviate somewhat from the measurements near the resonance may be due to correlations in the gas not captured in the mean field model. These results were reported in *Physical Review Letters* [14].

B.3 Novel Design for Unidirectional Operation of Ring Lasers

A technological advancement made during the course of this research was the development of a novel method to obtain uni-directional and single frequency operation of a ring laser that allows for higher output power than conventional means. We demonstrated this new technique with a diode-pumped solid-state laser operating at 1342 nm that could be frequency doubled to provide 671 nm light for laser cooling and trapping of lithium atoms.

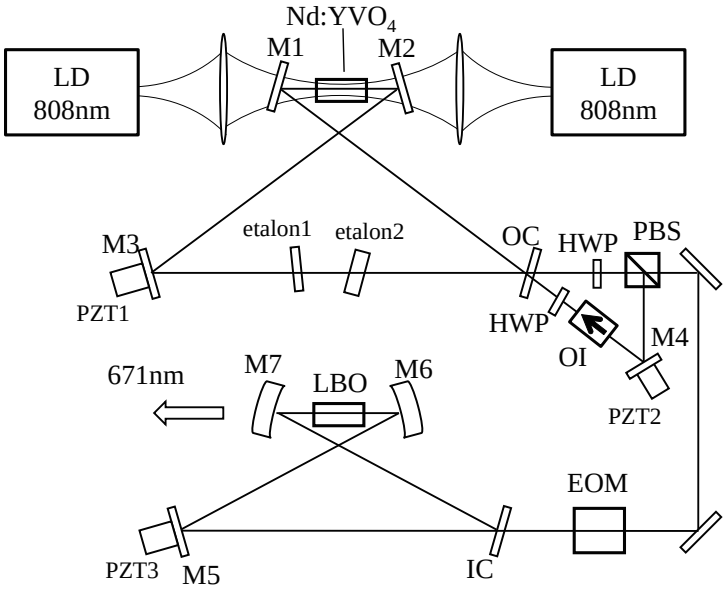

Figure 3: Self-injection locked, diode-pumped solid-state laser for laser cooling of Li atoms. The solid-state Nd:YVO_4 laser at the top consists of a bow-tie ring cavity that is weakly coupled to an external ring cavity containing an optical isolator which ensures unidirectional operation of the ring laser. The 1342 nm light output by the Nd:YVO_4 is frequency doubled by the non-linear LBO in the lower ring build up cavity. A total power of 800 mW at the 670.979, appropriate for cooling and trapping of ^{6}Li atoms, has been attained with this system and has been successfully used to produce quantum degenerate samples. Key: LD (laser diode), PZT (piezo-electric transducer), OC (output coupler), HWP (half-wave plate), OI (optical isolator), PBS (polarizing beam splitter), EOM (electro-optic modulator), and IC (input coupler).

Traditionally, uni-directional operation of a ring laser is achieved by inserting a Faraday rotator into the cavity in order to favor operation of one circulating mode over the other. However, insertion of a Faraday rotator reduces the achievable output power as these elements add significant loss in the optical cavity. We developed a novel approach to achieve uni-directional operation while maintaining high output power by putting an optical diode in an external ring cavity that is only weakly coupled to the primary ring cavity. Because only a small amount of optical power circulates in the external cavity, the loss introduced by the optical diode is significantly less detrimental.

A schematic of the laser system is shown in Fig. 3. The top-most bow-tie ring cavity is the primary cavity for the Nd:YVO_4 laser operating at 1342 nm. This primary cavity is weakly coupled

to an external ring cavity which contains an optical isolator. This external ring cavity only circulates a small fraction of the total power output by the laser (10's of milliWatts compared to several Watts) so that the loss introduced by the optical isolator does not significantly reduce the total achievable output power. The optical isolator is, however, effective at forcing uni-directional and single-frequency operation of the 1342 nm ring laser. This 1342 nm laser light can then by frequency doubled to provide laser cooling and trapping light for ^{6}Li atoms. This solid state laser system is an excellent alternative to diode laser/tapered amplifier systems. A total of 800 mW of light at 670.979 nm is achievable and the light produced is in a nearly pure TEM_{00} such that 76% of the light can be coupled into an optical fiber. We do not expect that this solid state laser system will age as tapered amplifier systems do and the lifetime of the system should be limited only by the lifetime of the 808 nm pump diode lasers (which should be $> 10,000$ hours and are readily replaced). A description of this laser system appeared in *Reviews of Scientific Instruments* [15]. (A result of this work also included a measurement of the Verdet constant for undoped YAG in the near infrared which appeared in *Optics Communications* [16].)

B.4 Relativistic Vortices in Bose-Einstein Condensates

Our interest in honeycomb lattices instigated a collaboration with Prof. Lincoln Carr and Laith Haddad from the Colorado School of Mines which focussed on relativistic phenomena that can be studied with ultracold atoms in a honeycomb lattice. Specifically, we have proposed a method to excite relativistic vortices in a Bose-Einstein condensate confined in a honeycomb lattice potential and have determined the stability of these vortices. Because the honeycomb lattice is a bi-partite lattice consisting of two interpenetrating triangular lattices (sub-lattices A and B), a condensate confined in a honeycomb lattice has a spinor structure associated with the sub-lattice degree of freedom. Further, for bosons condensed at a Dirac point in the band structure, low energy excitations obey a linear dispersion relation – like the dispersion relation for massless or ultra-relativistic particles. Ultimately, one can show that such a Bose-Einstein condensate with interactions can be described by a four-component Dirac spinor obeying a non-linear Dirac equation. This non-linear Dirac equation supports a wide variety of exotic vortex structures.

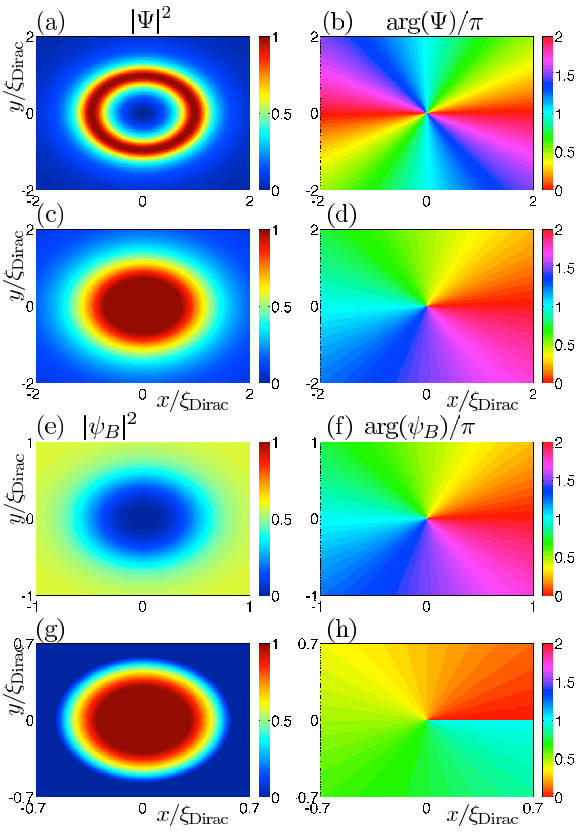

Figure 4: Subset of various relativistic vortex structures that can exist in the non-linear Dirac equation. Total density and phase of (a,b) $\ell = 2$ ring-vortex, (c,d) B sublattice of Mermin-Ho skyrmion, (e,f) ring-vortex/soliton, (g,h) half-quantum vortex, or semion.

We proposed a detailed method to excite relativistic vortices of various kinds. To excite a ring-vortex for example, a BEC is initially prepared at a Dirac point of the honeycomb lattice band structure having amplitude only in the A sublattice sites. Ring-vortices (a soliton-vortex pair) can be generated by transferring angular momentum to the BEC with a Laguerre-Gaussian laser beam and simultaneously modulating the lattice potential such that only the part of the condensate that acquires angular momentum makes a transition between sublattices. The stable vortex which results consists of a vortex in the B sublattice with a soliton in the A sublattice centered on the vortex core. We predict these ring-vortices will be stable for 1 – 10 seconds for realistic experimental parameters. A manuscript describing this work was published in *Physical Review A* [17].

B.5 Deformable, Site-Resolved Honeycomb Lattice

A central goal of this research program is to study fermionic atoms in the p-orbital band of a honeycomb optical lattice. To this end, we have implemented a 2D lattice honeycomb lattice which has a lattice constant sufficiently large that individual lattice sites can be optically resolved using off-the-shelf optics (see Fig. 5. The large lattice constant is achieved by forming the honeycomb lattice from 532 nm laser beams that intersect at a small angle. Single site resolution should allow for direct observation of Wigner crystallization and itinerant ferromagnetism, which had been identified as prominent collective phenomena to be observed in this research program. The figures shown in the upper right hand corner of Fig. 5 demonstrate single site resolution of the lattice potential. Further, by adjusting the amplitude, polarization and relative phase of the 532 nm laser beams we are able to continuously deform the lattice from a honeycomb lattice, to a dimerized honeycomb lattice, to a triangular lattice. As described in more detail below, this ability to deform the lattice potential will allow us to controllably introduce dispersion in the lowest p-orbital band of the honeycomb lattice.

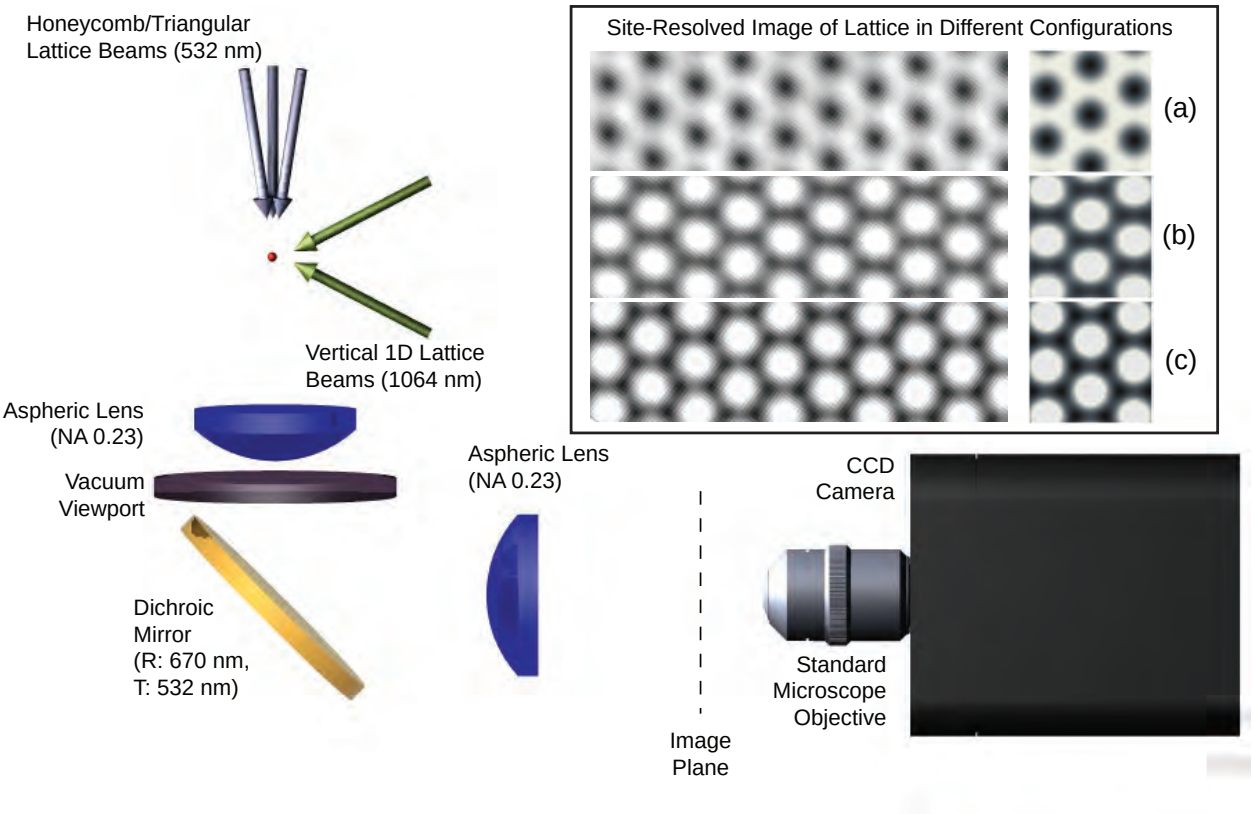

Figure 5: Site-Resolved Honeycomb/Triangular Lattice.

Fig. 5 shows the configuration of the 532 nm laser beams forming the deformable honeycomb/triangular lattice as well as the imaging system. In addition to the 532 nm laser beams, atoms are to be tightly confined vertically in a lattice formed from the two 1064 nm laser beams shown in light green to

produce a 3D lattice. Three 532 nm laser beams (light blue beams incident from above) form a long-period 2D lattice with either honeycomb or triangular geometry depending on the polarization of the beams. Owing to the large lattice constant, aspheric lenses with a numerical aperture of only 0.23 have sufficient resolution to image individual sites of the 2D lattices. The inset shows the two-dimensional optical lattice intensity pattern experienced by the atoms imaged through the optical system shown. The polarizations of the lattice beams are adjusted to form a (a) triangular, (b) intermediate, or (c) honeycomb lattice potential. Computer generated images for the corresponding configuration appear to the right. For the 2D lattices realized in these images, the triangular and honeycomb lattice geometries have a lattice site separation of $2.15\ \mu\mathrm{m}$ and $1.25\ \mu\mathrm{m}$ respectively. In order to image atoms in each site, a deep, short-period optical lattice will be turned on to hold each atom fixed in space while laser cooling light (not shown) is applied, causing the atoms to flouresce. The flourescence will be imaged onto a CCD array for 100's of ms to determine site occupation.

One of the goals of the originally proposed research program was to investigate itinerant ferromagnetism in the lowest p-orbital band of a honeycomb lattice, which is nearly dispersionless, and determine whether long-range ferromagnetic order persists as the dispersion is made non-zero. In order to controllably introduce dispersion in this system, we can deform the honeycomb lattice somewhat by making each pair of sites within a unit cell of the underlying triangular lattice become more strongly interacting. Adjusting the degree of dimerization will adjust the amount of dispersion.

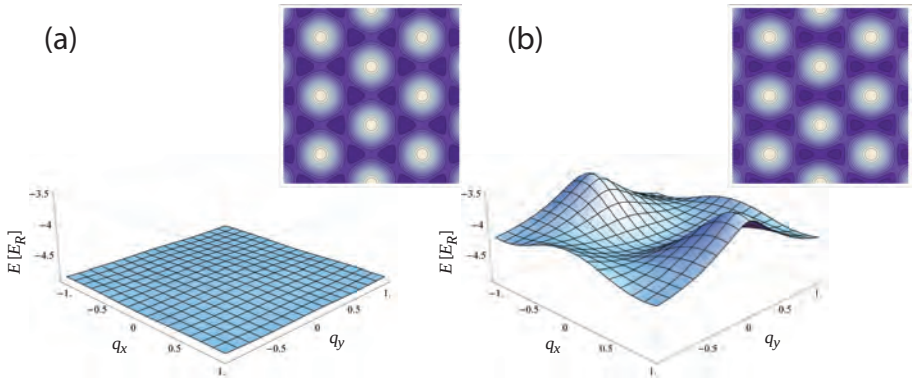

Figure 6: Controllably introducing dispersion into the lowest p-orbital band of a honeycomb lattice. (a) Dispersion for the lowest p-orbital band in the first Brillouin zone for the honeycomb lattice potential shown in the upper right corner. The width of the band is only $0.04\ E_R$ for a honeycomb lattice of $5\ E_R$ depth. (b) Dispersion for the lowest p-orbital band in the first Brillouin zone for the dimerized honeycomb lattice potential shown in the upper right corner where 15% of the power in the honeycomb lattice has been diverted to the triangular lattice. The width of the band is 20 times larger than in (a).

B.6 Confinement of ^{6}Li in a Two-Dimensional Triangular Lattice

In the third year of the award period, we demonstrated confinement of ^{6}Li atoms in a a two-dimensional triangular lattice. The vertical 1D lattice (to be produced by the 1064 nm laser beams shown in Fig. 5) has not yet been applied. The 2D lattice alone produces a 2D array of one-dimensional confining potentials. As described below, we have demonstrated that the fermionic ^{6}Li atoms are loaded into the ground band of the 2D triangular lattice potential.

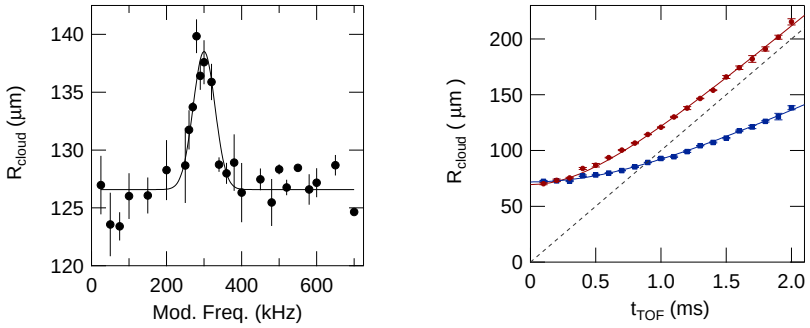

(a) Parametric Resonance (b) TOF from Lattice

Figure 7: Realization of 1D thermal gases of ^{6}Li fermions by confinement in a 2D triangular lattice. (a) Parametric resonance demonstrating that the oscillation frequency in the tight radial direction of each lattice site $\omega_\perp \simeq 2\pi \times 150\,\mathrm{kHz}$. (b) Time-of-flight expansion of ^{6}Li atoms from the 2D optical lattice. The clear anisotropic expansion of this non-interacting Fermi gas results from the fact that the zero-point energy in the radial direction of each tube (red) is larger than the thermal energy along the axis of the tube (blue) indicating that the 1D regime has been achieved. The dashed line shows the predicted expansion for a single tube occupying the harmonic oscillator ground state for $\omega_\perp = 2\pi \times 150\,\mathrm{kHz}$ (i.e. the dashed line corresponds to $R_{\mathrm{cloud}} = \sqrt{\frac{\hbar\omega_\perp}{m}}\, t_{\mathrm{TOF}}$).

When a gas is confined sufficiently tightly in two directions that the zero-point energy in the radial direction, $\hbar\omega_\perp$, is larger than all other energy scales in the system, i.e. $k_B T$, or $k_B T_F$ for a degenerate Fermi gas, then the Fermi gas is in the 1D regime. In Fig. 7, we demonstrate that we have confined a gas of ^{6}Li fermions sufficiently tightly in two directions to realize this regime. Fig. 7(a) shows our measurement of the radial oscillation frequencies in the tight direction of the tubes by the method of parametric resonance. Here the amplitude of the 2D lattice beams are modulated at the modulation frequency indicated on the horizontal axis. When the modulation frequency is twice the trap oscillation frequency, atoms are significantly heated. Thus, this data shows the trap oscillation frequency is $\omega_\perp = 2\pi \times 150\,\mathrm{kHz}$.

Fig. 7(b) shows time-of-flight expansion of the cloud following release from the lattice. The red filled circles show the radius of the cloud in the direction perpendicular to the axis of the 1D tubes (i.e. parallel to the tight radial directions of the individual 1D tubes) as a function of time of flight, t_{TOF}. The blue filled squares show the radius of the cloud in the direction parallel to the axis of the 1D tubes as a function of t_{TOF}. The red and blue lines are respectively fits to the data. Here the fit

to the axial expansion data (blue solid line) is a fit to $R_z = \sqrt{\frac{2k_BT}{m\omega_z^2}}\sqrt{1+\omega_z^2\,t_{\rm TOF}^2}$ allowing us to extract the apparent thermal temperature $T = 1.2\,\mu$K and the axial frequency $\omega_z = 2\pi \times 128\,$Hz. The red solid line, on the other hand, is a single parameter fit to $R_\perp = R_0\sqrt{1+v^2\,t_{\rm TOF}^2}$ where v is taken to be the velocity of expansion for the harmonic oscillator ground state wavefunction assuming $\omega_\perp = 2\pi \times 150\,$kHz, $v = \sqrt{\hbar\omega_\perp/m}$. The single fit parameter R_0 in this case is dependent on the number of tubes that are initially occupied in this direction. Thus, since this expansion asymptotes to the velocity of expansion for the harmonic oscillator ground state, we conclude that the atoms are predominately in the harmonic oscillator ground state in the radial direction of each tube. Furthermore, the very fact that this expansion is dramatically anisotropic indicates that the zero point energy in the radial direction is larger than the apparent thermal energy in the axial direction. From this data we indeed find that $k_B\,(1.2\,\mu{\rm K}) \ll \hbar\,(2\pi \times 150\,{\rm kHz})$ and the 1D regime has been achieved.

Having confined ^{6}Li fermions in the 2D lattice, we are now well positioned to apply a 1D lattice in the vertical direction and study ^{6}Li fermions in the p-orbital band of the honeycomb lattice. However, in the absence of the vertical lattice, the present system already allows us to study phenomena predicted for fermions in one-dimension.

One such phenomena, of interest for quantum metrology, is the preparation of multi-partite entanglement by inelastic s-wave collisions in a 1D Fermi gas. M. Foss-Feig *et al* citeRey2012 have shown that a 50/50 two-component mixture of fermions with an open inelastic s-wave channel will naturally evolve to a highly entangled state – the twin Fock state. This state has long been of interest since it is predicted to improve the accuracy of quantum metrology below the standard quantum limit. A Fermi gas with inelastic s-wave collisions naturally evolves to this state because it has a fully-antisymmetric spatial wavefunction and is therefore dark to inelastic s-wave collisions. M. Foss-Feig *et al* showed that in 1D it is the unique dark state. To create such an entangled state in our system, we need to controllably introduce inelastic s-wave collisions in a 50/50 two-state mixture. We do this by transferring one of the atoms in the 50/50 mixture to a different hyperfine state via a two-photon Raman transition and ensure that the newly created two-state mixture has an open inelastic s-wave channel. This is described in more detail below.

A second experiment we are pursuing in our 1D Fermi gases is the first observation of a distinguishing characteristic of the Fulde-Ferrell-Larkin-Ovchinikov (FFLO) superfluid phase – the observation of Cooper pairs with non-zero center of mass momenta. Indirect evidence for the FFLO phase in a polarized 1D Fermi gas was given by observing the spatial distribution of polarization in a trapped system to be opposite that for 3D gases and consistent with that predicted for 1D Fermi gases [18]. However, there is no definitive proof for the existence of the FFLO phase in this system. In our experiment we are attempting to provide this proof by observing quantum noise correlations in the time-of-flight absorption images that demonstrate Cooper pairing correlations for Cooper pairs that have a non-zero center of mass momentum. For the time-of-flight absorption images to show these correlations, the atoms must expand ballistically during the time-of-flight. What is unique about our experiment is that we have developed a method to rapidly extinguish interactions in a Fermi gas by transferring atoms to a very weakly interacting two-state mixture using a Raman

transition. By transferring atoms from a strongly to a weakly interacting mixture simultaneous with eliminating confinement along the 1D tubes, we will be able to attain a faithful reconstruction of the momentum distribution in the tubes. Correlations in these momentum distributions should give direct evidence for Cooper pairs with a non-zero center-of-mass momentum. In the following section we describe the method we have developed for rapidly controlling interactions in a Fermi gas. This allows us to either rapidly induce inelastic s-wave collisions, for preparing a twin Fock state as described above, or rapidly extinguish interactions in a strongly interact two-component Fermi gas, useful for quantum noise interferometry experiments.

B.7 Rapid Control of Interactions in a Two-Component ^{6}Li Gas

We have developed a novel technique for the rapid control of interactions in a two-component ^{6}Li gas based on driving two-photon Raman transition between different internal states of ^{6}Li. This allows us to rapidly change a two-component mixture from one that is strongly interacting to one that is essentially non-interacting. This can be useful for reconstructing the initial momentum distribution of atoms in the trap by time-of-flight imaging if interactions are extinguished simultaneously with release of atoms from the trap. This would then open up the possibility of novel techniques for characterizing strongly correlated phases of ^{6}Li atoms such as quantum noise interferometry [19] or momentum-resolved photo-emission spectroscopy [20]. Alternatively, if so desired, one can rapidly produce a two-component mixture with large inelastic two-body loss rates starting from a stable, strongly-interacting mixture. This can be useful for probing local spin correlations or for preparing multi-partite entangled states in the steady-state which arises naturally for a thermal, two-component Fermi gas when an s-wave inelastic loss channel exists [21].

To accomplish these goals we have demonstrated that we can transfer atoms between different internal hyperfine states of ^{6}Li such that certain two-component mixtures are weakly interacting, while others are strongly interacting, while other mixtures decay rapidly by two body inelastic collisions. In order for us to consider the scattering properties of different two-state mixtures of ^{6}Li, we use an extremely simple model of the $^6Li_2$ singlet and triplet molecular potentials (treating them simply as square well potentials) and perform full coupled-channel s-wave scattering calculations with these simplistic model potential.

Each possible two-state mixture of the three lowest hyperfine states, states $|1\rangle$, $|2\rangle$ and $|3\rangle$, have no allowed spin-exchange decay channels and each exhibits a broad Feshbach resonance. Thus, these three mixtures are each very well suited to provide strongly interacting mixtures with zero or minimal two-body loss. Among these, the $|1\rangle - |2\rangle$ mixture is the best of these since even a dipolar loss rate, provided p-wave collisions are frozen out, is forbidden for this mixture. Still, the $|1\rangle - |3\rangle$ mixture and the $|2\rangle - |3\rangle$ mixtures have been observed to be quite stable with relatively small dipolar relaxation rate constants.

For the realization of twin Fock states and as a diagnostic tool for itinerant ferromagnetism, we are interested in identifying two-state mixtures with large spin-exchange decay rates. Two-state mixtures that involve one atom from states $|1\rangle$, $|2\rangle$, or $|3\rangle$ and one atom from states $|4\rangle$, $|5\rangle$, or

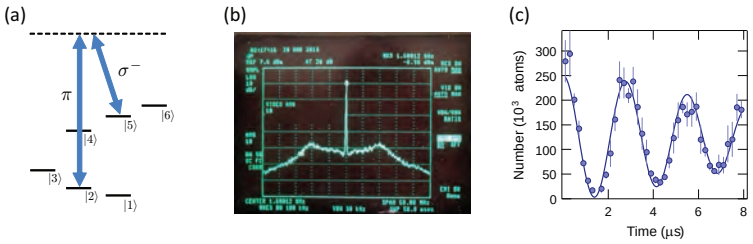

Figure 8: Two-photon Raman transition used to rapidly control interactions in ^{6}Li gas by quickly switching between different two-state mixtures. (a) Two-photon Raman transition transfers population between states $|2\rangle$ and $|5\rangle$. In this case, if a strongly interaction $|1\rangle - |2\rangle$ mixture initially exists, transfer of population from state $|2\rangle$ to state $|5\rangle$ produces a $|1\rangle - |5\rangle$ mixture which is weakly interacting and relatively stable against decay. (b) Beat note between two diode lasers driving the Raman transition as recorded by a spectrum analyzer. (c) Rabi oscillations between states $|2\rangle$ and $|5\rangle$. The decay of contrast is due to the finite size of the Raman beams.

$|6\rangle$ are particularly appealing since we can then, starting from a stable two state mixture, create a decaying two state mixture by transferring one atom from either state $|1\rangle$, $|2\rangle$, or $|3\rangle$ to state $|4\rangle$, $|5\rangle$, or $|6\rangle$. In practice, we transfer population between two different hyperfine states by driving a two-photon Raman transition (see Fig. 8(a)).

The Raman transition is driven by two phase locked diode lasers. The servo bandwidth of the phase lock is $\simeq 10\,\mathrm{MHz}$. The beat note signal between the lasers recorded by a spectrum analyzer is shown in Fig. 8(b). Since the difference frequency between the states tunes as $\simeq 2.8\,\mathrm{MHz/G}$ and we typically operate at fields between 500 and 850 G, the required difference frequency between the lasers ranges from $1.4 - 2.4\,\mathrm{GHz}$. Fig. 8(c) shows a typical Rabi oscillation between two different hyperfine states in ^{6}Li. The solid curve shows the expected decay of contrast due to the finite size of our Raman beams and the spatial extent of the atomic cloud which causes dephasing due to an inhomogeniety in Raman Rabi frequencies. Expansion of the Raman beams in one direction only (since the atomic cloud is already small in the orthogonal direction) should reduce the decay of contrast with only a modest reduction of achievable Rabi frequencies. The stability of our applied magnetic field (rms fluctuations $\leq 1\,\mathrm{mG}$) is sufficient to allow us to drive these Raman transitions coherently despite the fact that this is a field sensitive transition.

Using our simplified coupled-channel calculation, we have identified several two-state mixtures with large spin-exchange decay rate constants and have experimentally measured the two-body loss rate coefficients in several cases. The predicted and experimentally measured two-body spin-exchange decay rate constants K_2 for a two-state $|2\rangle - |5\rangle$ mixture and a two-state $|2\rangle - |6\rangle$ mixture are shown in Fig. 9. In each case, the density of atoms in state $|2\rangle$ decays according to $\dot{n}_2 = -\Gamma n_2 - K_2\, n_2\, n_x$ where Γ is the one-body loss coefficient due to background gas collisions (independently measured to be $\Gamma = 0.08\,\mathrm{s}^{-1}$ in our system) and n_x is the density in the other spin state (i.e. either n_5 or n_6, depending on the mixture). The densities are computed from measured values of the atom number in each state, the trap frequencies, and the tem-

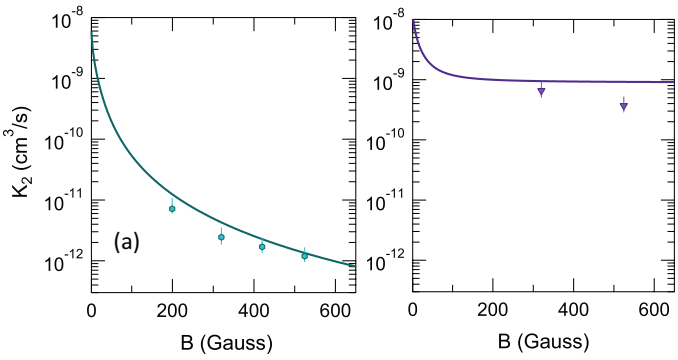

Figure 9: Predicted and measured spin-exchange loss rate coefficients for a $|2\rangle - |5\rangle$ mixture and for a $|2\rangle - |6\rangle$ mixture. (a) The spin-exchange loss rate coefficient predicted by a simple model (solid line) for a $|2\rangle - |5\rangle$ mixture in comparison to measured values. (b) Predicted and measured spin-exchange loss rate coefficient for a $|2\rangle - |6\rangle$ mixture.

perature. In each case, the measured values were determined from thermal gases at densities $n_2 \simeq n_x \simeq 2.5 \times 10^{13}\,\mathrm{atoms/cm^3}$. The predicted spin-exchange coefficients are shown as solid lines. The predictions of our simple model and measured values show good agreement. Both the $|2\rangle - |5\rangle$ and $|2\rangle - |6\rangle$ are well-suited for creation of twin Fock states or as a diagnostic tool for measuring local spin correlations in a ferromagnetic phase.

We are also interested in identifying two-state mixtures that are relatively stable (i.e. K_2 is small) and are also weakly interacting. Such a mixture will be useful for rapidly extinguishing interactions in a two-component Fermi gas if a strongly-interacting two-state mixture can suddenly be changed to a weakly interacting two-state mixture by transferring population in one of the two states from one hyperfine component to another. For example, if we start from a mixture of atoms in states $|1\rangle$ and $|2\rangle$, which can be made strongly interacting by utilizing the broad Feshbach resonance which occurs at a field of 832.2 G [22], suddenly transferring population from state $|2\rangle$ to state $|5\rangle$ (see Fig. 8(a)) would rapidly eliminate interactions in the two-component Fermi gas provided that the $|1\rangle - |5\rangle$ mixture is weakly interacting. Further, the $|1\rangle - |5\rangle$ mixture should be relatively stable since s-wave inelastic spin-exchange collisions are forbidden if even a modest bias field is applied, though a small dipolar loss rate may occur. Using our simple coupled-channels calculation, we find that the predicted s-wave scattering length for fields $> 500\,\mathrm{G}$ is $a_{15} \lesssim 10\,a_0$ (see Fig. 10(a)). The shaded region shows a range of values of a_{15} for different model parameters used in our simple coupled-channel calculation that get either the binding energy of the highest singlet molecular state correct or the location of the various Feshbach resonances correct. Note that for a scattering length of $a_{15} = 10\,a_0$ in a gas at a density of $n_1 = n_5 = 10^{13}\,\mathrm{atoms/cm^3}$ which we might expect to achieve in the 1D tubes, the mean free path for atoms $\ell_{\mathrm{mfp}} = \frac{1}{n\,\sigma} = \frac{1}{n\,4\pi a_{15}^2} = 2.8\,\mathrm{cm}$. Thus, if strong interactions were extinguished by transferring atoms to this mixture simultaneously with eliminating the trapping potential, the atoms would be free to ballistically expand even if they are at an initial density of $n_1 = n_5 = 10^{13}\,\mathrm{atoms/cm^3}$.

As noted above, the spin-exchange loss rate (in the presence of even a small bias field) is ex-

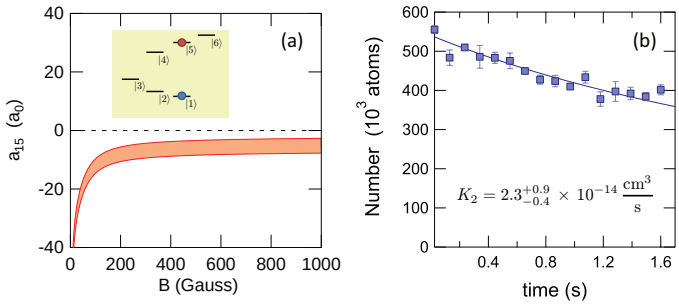

Figure 10: Stable, weakly-interacting two-state mixture of ^{6}Li fermions. (a) The s-wave scattering length a_{15} for a $|1\rangle - |5\rangle$ mixture of ^{6}Li atoms as a function of field as predicted by a simple coupled channels model. The range of scattering lengths shown are for different choices of model parameters. (b) Decay of the $|1\rangle - |5\rangle$ mixture in a gas with an initial density of $2.5 \times 10^{13}\,\mathrm{atoms/cm}^3$ in each spin state. The decay is due to a weak dipolar loss with a measured two-body inelastic loss rate coefficient $K_2 = 2.3^{+0.9}_{-0.4} \times 10^{-14}\mathrm{cm}^3/\mathrm{s}$.

actly zero for the $|1\rangle - |5\rangle$ mixture. However, due to weak magnetic dipole-dipole interactions between the alkali atoms, a small dipolar relaxation rate constant may exist. To determine the two-body loss rate coefficient K_2 for the $|1\rangle - |5\rangle$ mixture, we have measured the decay of atoms confined in a crossed dipole trap at an initial density of $n_1 = n_5 = 2.5 \times 10^{13}\,\mathrm{atoms/cm}^3$ (see Fig. 10(b)). From fitting the decay using $\dot{n}_1 = -\Gamma n_1 - K_2\, n_1\, n_5$, we find the loss rate coefficient $K_2 = 2.3^{+0.9}_{-0.4} \times 10^{-14}\mathrm{cm}^3/\mathrm{s}$. Note that this weak loss rate constant due to dipole-dipole interactions is approximately two orders of magnitude smaller than the lowest spin-exchange loss rate coefficient we measured in Fig. 9. A 50/50 mixture of atoms in this mixture at a density $n_1 = n_5 = 10^{13}\,\mathrm{atoms/cm}^3$ would decay over a time scale of seconds. Thus, the $|1\rangle - |5\rangle$ mixture is well suited for making a weakly interacting mixture for time-of-flight expansion, since expansion times of $\lesssim 10\,\mathrm{ms}$ are typically used in the case of ^{6}Li.

References

[1] C. H. Schunck, M. W. Zwierlein, C. A. Stan, S. M. F. Raupach, W. Ketterle, A. Simoni, E. Tiesinga, C. J. Williams, and P. S. Julienne, "Feshbach resonances in fermionic ^{6}Li," *Phys. Rev. A* **71**, 045601 (2005).

[2] G. K. Campbell, M. M. Boyd, J. W. Thomsen, M. J. Martin, S. Blatt, M. D. Swallows, T. L. Nicholson, T. Fortier, C. W. Oates, S. A. Diddams, N. D. Lemke, P. Naidon, P. Julienne, J. Ye, and A. D. Ludlow, "Probing interactions between ultracold fermions," *Science* **324**, 360–363 (2009).

[3] N. D. Lemke, J. von Stecher, J. A. Sherman, A. M. Rey, C. W. Oates, and A. D. Ludlow, "p-wave cold collisions in an optical lattice clock," *Phys. Rev. Lett.* **107**, 103902 (2011).

[4] K. Gibble, "Decoherence and collisional frequency shifts of trapped bosons and fermions," *Phys. Rev. Lett.* **103**, 113202 (2009).

[5] K. Gibble, and B. J. Verhaar, "Eliminating cold-collision frequency shifts," *Phys. Rev. A* **52**, 3370–3373 (1995).

[6] S. Gupta, Z. Hadzibabic, M. Zwierlein, C. Stan, K. Dieckmann, C. Schunck, E. van Kempen, B. Verhaar, and W. Ketterle, "Radio-frequency spectroscopy of ultracold fermions," *Science* **300**, 1723–1726 (2003).

[7] M. W. Zwierlein, Z. Hadzibabic, S. Gupta, and W. Ketterle, "Spectroscopic insensitivity to cold collisions in a two-state mixture of fermions," *Phys. Rev. Lett.* **91**, 250404 (2003).

[8] A. M. Rey, A. V. Gorshkov, and C. Rubbo, "Many-body treatment of the collisional frequency shift in fermionic atoms," *Phys. Rev. Lett.* **103**, 260402 (2009).

[9] Z. Yu, and C. J. Pethick, "Clock shifts of optical transitions in ultracold atomic gases," *Phys. Rev. Lett.* **104**, 010801 (2010).

[10] M. J. Martin, M. Bishof, M. D. Swallows, X. Zhang, C. Benko, J. von Stecher, A. V. Gorshkov, A. M. Rey, and J. Ye, "A quantum many-body spin system in an optical lattice clock," *Science* **341**, 632–636 (2013).

[11] E. L. Hazlett, Y. Zhang, R. W. Stites, K. Gibble, and K. M. O'Hara, "s-Wave Collisional Frequency Shift of a Fermion Clock," *Phys. Rev. Lett.* **110**, 160801 (2013).

[12] A. Schwenk, and C. J. Pethick, "Resonant fermi gases with a large effective range," *Phys. Rev. Lett.* **95**, 160401 (2005).

[13] M. J. H. Ku, A. T. Sommer, L. W. Cheuk, and M. W. Zwierlein, "Revealing the superfluid lambda transition in the universal thermodynamics of a unitary fermi gas," *Science* **335**, 563–567 (2012).

[14] E. L. Hazlett, Y. Zhang, R. W. Stites, and K. M. O'Hara, "Realization of a resonant fermi gas with a large effective range," *Phys. Rev. Lett.* **108**, 045304 (2012).

[15] Y. Miake, T. Mukaiyama, K. M. O'Hara, and S. Gensemer, "A self-injected, diode-pumped, solid-state ring laser for laser cooling of Li atoms," *Rev. Sci. Inst.* **86**, (2015).

[16] R. W. Stites, and K. M. O'Hara, "The Verdet constant of undoped Y_3 Al_5 O_{12} in the near infrared," *Opt. Commun.* **285**, 3997–4000 (2012).

[17] L. H. Haddad, K. M. O'Hara, and L. D. Carr, "Nonlinear dirac equation in bose-einstein condensates: Preparation and stability of relativistic vortices," *Phys. Rev. A* **91**, 043609 (2015).

[18] Y. A. Liao, A. S. C. Rittner, T. Paprotta, W. H. Li, G. B. Partridge, R. G. Hulet, S. K. Baur, and E. J. Mueller, "Spin-imbalance in a one-dimensional fermi gas," *Nature* **467**, 567–U86 (2010).

[19] E. Altman, E. Demler, and M. D. Lukin, "Probing many-body states of ultracold atoms via noise correlations," *Phys. Rev. A* **70**, 013603 (2004).

[20] J. T. Stewart, J. P. Gaebler, and D. S. Jin, "Using photoemission spectroscopy to probe a strongly interacting Fermi gas," *Nature* **454**, 744 (2008).

[21] M. Foss-Feig, A. J. Daley, J. K. Thompson, and A. M. Rey, "Steady-state many-body entanglement of hot reactive fermions," *Physical Review Letters* **109**, (2012).

[22] G. Zürn, T. Lompe, A. N. Wenz, S. Jochim, P. S. Julienne, and J. M. Hutson, "Precise characterization of Li-6 feshbach resonances using trap-sideband-resolved rf spectroscopy of weakly bound molecules," *Phys. Rev. Lett.* **110**, 135301 (2013).

C Personnel

The research staff who has worked on this project over the course of the award period consists of:

Principle Investigator: Prof. Kenneth OHara
Postdoctoral Research Associate: Dr. Chenglin Cao
Graduate Student: Francisco Fonta
Graduate Student: Eric Hazlett
Graduate Student: Andrew Marcum
Graduate Student: Arif Mawardi Bin Ismail
Graduate Student: Ronald Stites
Graduate Student: Yi Zhang

D Publications

- R. W. Stites and K. M. OHara, "The Verdet Constant of Undoped $Y_3Al_5O_{12}$ in the Near Infrared," Opt. Comm. **285**, 3997, (2012).

- E. L. Hazlett, Y. Zhang, R. W. Stites, and K. M. OHara, "Realization of a Resonant Fermi Gas with a Large Effective Range," Phys. Rev. Lett. **108**, 045304 (2012).

- E. L. Hazlett, Y. Zhang, R. W. Stites, K. Gibble, and K. M. OHara, "s-Wave Collisional Frequency Shift of a Fermion Clock," Phys. Rev. Lett. **110**, 160801 (2013).

- L. H. Haddad, K. M. O'Hara, and L. D. Carr, "Nonlinear Dirac equation in Bose-Einstein condensates: Preparation and stability of relativistic vortices," Phys. Rev. A **91**, 043609 (2015).

- Y. Miake, T. Mukaiyama, K. M. O'Hara, S. Gensemer, "A self-injected, diode-pumped, solid-state ring laser for laser cooling of Li atoms," Rev. Sci. Instrum. **86**, 043113 (2015).

E Interactions/Transitions

Presentations at Meetings, Conferences, and Universities

- *Modeling Nuclei and Neutron Matter with Ultracold Atoms*; Cornell University, Laboratory of Atomic and Solid State Physics Seminar on August 30, 2011.
- *Modeling Nuclei and Neutron Matter with Ultracold Atoms*, University of Notre Dame, Physics Colloquium on September 14, 2011.
- *Measuring the Collisional Frequency Shift in a Fermi Gas*, University of Maryland, Joint Quantum Institute Seminar on September 19, 2011.
- *Modeling Nuclei and Neutron Matter with Ultracold Atoms*, The Pennsylvania State University, Physics Colloquium on September 29, 2011.
- *Measuring the Collisional Frequency Shift in a Fermi Gas*, Georgia Institute of Technology, Georgia Tech Quantum Institute Seminar on November 14, 2011.
- *The Eimov Effect in a Fermi Gas*, 42nd Winter Colloquium on the Physics of Quantum Electronics, Snowbird, UT on Jan. 5, 2012.
- *Realization of a Resonant Fermi Gas with a Large Effective Range*, American Physical Society, DAMOP, June 6, 2012.
- s*-Wave Clock Shift for Fermions*, American Physical Society, DAMOP, June 7, 2012.
- s*-Wave Collisional Frequency Shift of a Fermion Clock,* European Frequency and Time Forum & International Frequency Control Symposium (EFTF/IFC), 2013 Joint, 1025 (2013).
- *Observing, Understanding, then Eliminating Cold Collision Frequency Shifts in Fermi-Based Atomic Clocks*, Institute of Quantum Optics & Quantum Information, Innsbruck, on May 8, 2014.
- *Observing, Understanding, then Eliminating Cold Collision Frequency Shifts in Fermi - Based Atomic Clocks*, University of Toronto, Seminar on July 10, 2014.

F Inventions

None during this grant period.

G Awards

None during this grant period.

1.

1. Report Type

Final Report

Primary Contact E-mail

Contact email if there is a problem with the report.

kohara@phys.psu.edu

Primary Contact Phone Number

Contact phone number if there is a problem with the report

814-865-7259

Organization / Institution name

The Pennsylvania State University

Grant/Contract Title

The full title of the funded effort.

Ultracold Fermions in the P-Orbital Band of an Optical Lattice

Grant/Contract Number

AFOSR assigned control number. It must begin with "FA9550" or "F49620" or "FA2386".

FA9550-11-1-0161

Principal Investigator Name

The full name of the principal investigator on the grant or contract.

Kenneth M. O'Hara

Program Manager

The AFOSR Program Manager currently assigned to the award

Tatjana Curcic

Reporting Period Start Date

07/15/2011

Reporting Period End Date

03/31/2015

Abstract

The goal of this research program is to investigate strongly-correlated many-body phases that emerge when interacting fermions occupy the p-orbital band of an optical lattice. Progress made toward this objective included demonstration of a site-resolved, continuously deformable two-dimensional honeycomb/triangular lattice and loading of Li-6 atoms into a triangular configuration of lattice beams. Further, a novel solid state laser source for 671 nm light was developed and new methods for rapidly controlling interactions between fermionic Li-6 atoms were demonstrated. While making this progress, scientific opportunities arose to make discoveries in other research areas of interest to the AFOSR. Specifically, the scope of the project was broadened to include studies of s-wave collisional frequency shifts in an ultracold Fermi gas (relevant for improving/characterizing the accuracy of next generation atomic clocks), the realization of momentum dependent s-wave interactions in a Fermi gas (relevant for quantum simulation), and the realization of multi-partite entangled states by dissipative exothermic collisions in a one-dimensional Fermi gas (relevant for quantum metrology).

Distribution Statement

This is block 12 on the SF298 form.

Distribution A - Approved for Public Release

Explanation for Distribution Statement

If this is not approved for public release, please provide a short explanation. E.g., contains proprietary information.

SF298 Form

Please attach your SF298 form. A blank SF298 can be found here. Please do not password protect or secure the PDF The maximum file size for an SF298 is 50MB.

AFOSR_FinalPerfRep_FA9550_11_1_0161_SF298.pdf

Upload the Report Document. File must be a PDF. Please do not password protect or secure the PDF . The maximum file size for the Report Document is 50MB.

AFOSR_FinalPerfRep_FA9550_11_1_0161.pdf

Upload a Report Document, if any. The maximum file size for the Report Document is 50MB.

Archival Publications (published) during reporting period:

R. W. Stites and K. M. OHara, "The Verdet Constant of Undoped Y3Al5O12 in the Near Infrared," Opt. Comm. 285, 3997, (2012).

E. L. Hazlett, Y. Zhang, R. W. Stites, and K. M. OHara, "Realization of a Resonant Fermi Gas with a Large Effective Range," Phys. Rev. Lett. 108, 045304 (2012).

E. L. Hazlett, Y. Zhang, R. W. Stites, K. Gibble, and K. M. OHara, "s-Wave Collisional Frequency Shift of a Fermion Clock," Phys. Rev. Lett. 110, 160801 (2013).

L. H. Haddad, K. M. O'Hara, and L. D. Carr, "Nonlinear Dirac equation in Bose-Einstein condensates: Preparation and stability of relativistic vortices," Phys. Rev. A 91, 043609 (2015).

Y. Miake, T. Mukaiyama, K. M. O'Hara, S. Gensemer, "A self-injected, diode-pumped, solid-state ring laser for laser cooling of Li atoms," Rev. Sci. Instrum. 86, 043113 (2015).

Changes in research objectives (if any):

Change in AFOSR Program Manager, if any:

Extensions granted or milestones slipped, if any:

AFOSR LRIR Number

LRIR Title

Reporting Period

Laboratory Task Manager

Program Officer

Research Objectives

Technical Summary

Funding Summary by Cost Category (by FY, $K)

	Starting FY	FY+1	FY+2
Salary			
Equipment/Facilities			
Supplies			
Total			

Report Document

Report Document - Text Analysis

Report Document - Text Analysis

Appendix Documents

2. Thank You

E-mail user

Jul 27, 2015 17:13:15 Success: Email Sent to: kohara@phys.psu.edu